

See discussions, stats, and author profiles for this publication at: <https://www.researchgate.net/publication/231242329>

# Highly Ordered Magnetic Ceramic Nanorod Arrays from a Polyferrocenylsilane by Nanoimprint Lithography with Anodic Aluminum Oxide Templates

ARTICLE *in* CHEMISTRY OF MATERIALS · MAY 2009

Impact Factor: 8.35 · DOI: 10.1021/cm900164b

---

CITATIONS

21

---

READS

10

4 AUTHORS, INCLUDING:



Kun Liu

University of Toronto

36 PUBLICATIONS 1,144 CITATIONS

SEE PROFILE

# Highly Ordered Magnetic Ceramic Nanorod Arrays from a Polyferrocenylsilane by Nanoimprint Lithography with Anodic Aluminum Oxide Templates

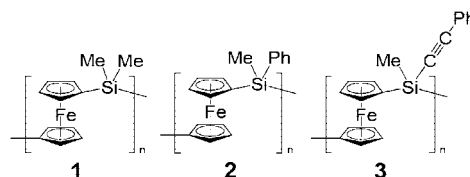
Kun Liu,<sup>†</sup> Sébastien Fournier-Bidoz,<sup>†</sup>  
Geoffrey A. Ozin,<sup>\*,†</sup> and Ian Manners<sup>\*,‡</sup>

The School of Chemistry, University of Bristol, Bristol BS8  
ITS, United Kingdom, and Department of Chemistry,  
University of Toronto, Toronto, Canada M5S 3H6

Received January 19, 2009

Ordered arrays of magnetic nanostructures have attracted intense academic and industrial interest, due to their unique physical traits and widespread technological applications in areas such as biosensors, spintronics, magnetic random access memory (MRAM), and patterned recording media.<sup>1–5</sup> Conventional methods for their fabrication include, for example, electron-beam lithography,<sup>6</sup> photolithography,<sup>7</sup> dip-pen nanolithography,<sup>8</sup> and soft lithography.<sup>9</sup> Most of these techniques involve multiple steps and expensive instrumentation. Block copolymer lithography is a bottom-up facile method for creating large area nanoscale patterns,<sup>10,11</sup> however, magnetic nanostructures with high aspect ratio are difficult to obtain with this method. Nanoimprint lithography (NIL)<sup>12</sup> with hard masks, such as nanoporous anodic aluminum oxide (AAO) templates, is an alternative technique for high-throughput patterning of polymer nanostructures with great precision and at low cost.<sup>13</sup> NIL using AAO templates relies on direct thermal infiltration of the polymer resist into nanochannels and can therefore achieve resolutions beyond the limitations set by light diffraction or beam scattering in conventional lithography methods. Up to now, researchers have mostly used commercial thermoplastic materials, e.g., polystyrene and poly(methylmethacrylate), or

Scheme 1. Polyferrocenylsilanes (PFSs)



siloxane copolymers as NIL resists. However, these materials are sacrificial in most cases and clearly do not allow access to magnetic nanostructures.

Polyferrocenylsilanes (PFSs) (e.g., **1**, **2**, and **3** in Scheme 1) are an interesting class of processable high-molecular-weight metallopolymer that are readily accessible by ring-opening polymerization routes and possess a range of intriguing properties as a result of the presence of inorganic elements of Fe and Si in the backbone (Scheme 1).<sup>14</sup> One interesting feature is their ability to act as high yield pyrolytic precursors to C/SiC ceramics containing Fe nanoparticles (NPs).<sup>15,16</sup> In this work, we focused on the use of a PFS with pendant acetylenic substituents (**3**) that showed the highest ceramic yield to date determined by thermogravimetric analysis (TGA) among uncrosslinked PFS homopolymers.<sup>17,18</sup> In addition, easy processing and air- and moisture-stability make PFS **3** an excellent potential polymer resist for nanoimprinting processes.

In this communication, we describe a simple method to fabricate large area highly ordered arrays of magnetic ceramic

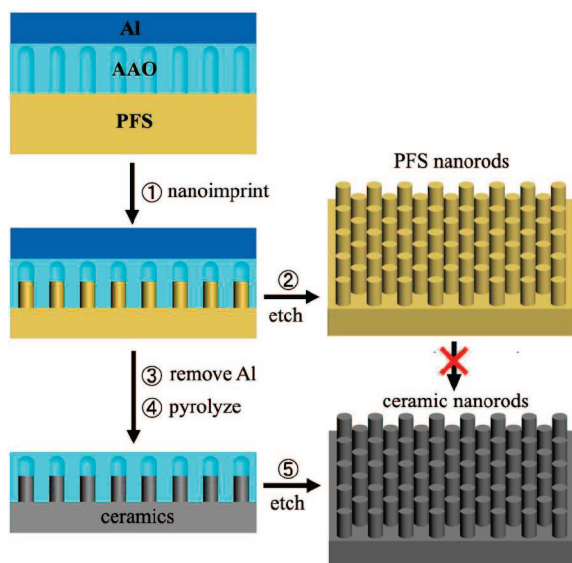
\* Corresponding author. E-mail: Ian.Manners@bristol.ac.uk (I.M.); gozin@chem.utoronto.ca (G.A.O.).

<sup>†</sup> University of Toronto.

<sup>‡</sup> University of Bristol.

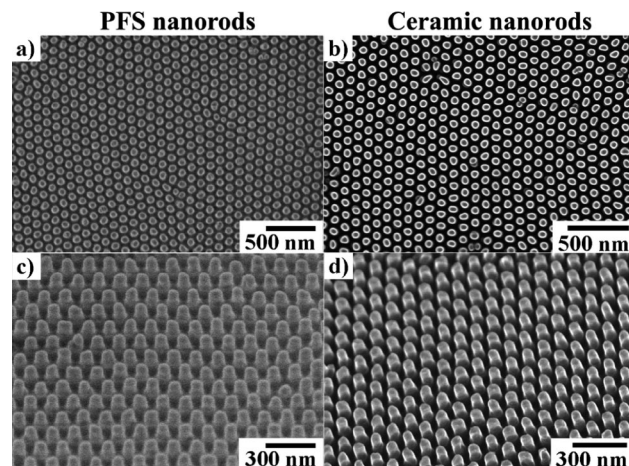
- (1) Martín, J. I.; Nogués, J.; Liu, K.; Vicent, J. L.; Schuller, I. K. *J. Magn. Magn. Mater.* **2003**, *256*, 449–501.
- (2) Edelstein, R. L.; Tamanaha, C. R.; Sheehan, P. E.; Miller, M. M.; Baselt, D. R.; Whitman, L. J.; Colton, R. J. *Biosens. Bioelectron.* **2000**, *14*, 805–813.
- (3) Prinz, G. A. *Science* **1998**, *282*, 1660–1663.
- (4) Wolf, S. A.; Awschalom, D. D.; Buhrman, R. A.; Daughton, J. M.; von Molnár, S.; Roukes, M. L.; Chtchelkanova, A. Y.; Treger, D. M. *Science* **2001**, *294*, 1488–1495.
- (5) Ross, C. A. *Annu. Rev. Mater. Res.* **2001**, *31*, 203–235.
- (6) Wei, M. S.; Chou, S. Y. *J. Appl. Phys.* **1994**, *76*, 6679–6681.
- (7) Wallraff, G. M.; Hinsberg, W. D. *Chem. Rev.* **1999**, *99*, 1801–1822.
- (8) Piner, R. D.; Zhu, J.; Xu, F.; Hong, S.; Mirkin, C. A. *Science* **1999**, *283*, 661–663.
- (9) Gates, B. D.; Xu, Q.; Stewart, M.; Ryan, D.; Willson, C. G.; Whitesides, G. M. *Chem. Rev.* **2005**, *105*, 1171–1196.
- (10) Hawker, C. J.; Russell, T. P. *MRS Bull.* **2005**, *30*, 952–966.
- (11) For an approach to magnetic NRs using PFS block copolymers see: Rider, D. A.; Liu, K.; Eloi, J.-C.; Vanderark, L.; Yang, L.; Wang, J.-Y.; Grozea, D.; Lu, Z.-H.; Russell, T. P.; Manners, I. *ACS Nano* **2008**, *2*, 263–270.
- (12) (a) Chou, S. Y.; Krauss, P. R.; Renstrom, P. J. *J. Appl. Phys. Lett.* **1995**, *67*, 3114–3116. (b) Guo, L. J. *Adv. Mater.* **2007**, *19*, 495–513.
- (13) (a) Lee, W.; Lee, J.-K. *Adv. Mater.* **2002**, *14*, 1187–1190. (b) Moon, S. I.; McCarthy, T. J. *Macromolecules* **2003**, *36*, 4253–4255.

- (14) (a) Manners, I. *Science* **2001**, *294*, 1664–1666. (b) Whittell, G. R.; Manners, I. *Adv. Mater.* **2007**, *19*, 3439–3468. (c) Bellas, V.; Rehahn, M. *Angew. Chem., Int. Ed.* **2007**, *46*, 5082–5104. (d) Korczagin, I.; Lammertink, R. G. H.; Hempenius, M. A.; Golze, S.; Vancso, G. J. *Adv. Polym. Sci.* **2006**, *200*, 91–117. (e) Hong, S. W.; Xu, J.; Xia, J.; Lin, Z.; Qiu, F.; Yang, Y. *Chem. Mater.* **2005**, *17*, 6223–6226. (f) Pannell, K. H.; Imshennik, V. I.; Maksimov, Yu. V.; Il'ina, M. N.; Sharma, H. K.; Papkov, V. S.; Suzdalev, I. P. *Chem. Mater.* **2005**, *17*, 1844–1850.
- (15) (a) MacLachlan, M. J.; Ginzburg, M.; Coombs, N.; Coyle, T. W.; Raju, N. P.; Greedan, J. E.; Ozin, G. A.; Manners, I. *Science* **2000**, *287*, 1460–1463. (b) Ginzburg, M.; MacLachlan, M. J.; Yang, S. M.; Coombs, N.; Coyle, T. W.; Raju, N. P.; Greedan, J. E.; Herber, R. H.; Ozin, G. A.; Manners, I. *J. Am. Chem. Soc.* **2002**, *124*, 2625–2639. (c) MacLachlan, M. J.; Ginzburg, M.; Coombs, N.; Raju, N. P.; Greedan, J. E.; Ozin, G. A.; Manners, I. *J. Am. Chem. Soc.* **2000**, *122*, 3878–3891.
- (16) For the works of other groups on the use of PFS and other metallopolymer to prepare metal NPs based materials via pyrolysis see: (a) Sun, Q.; Lam, J. W. Y.; Xu, K.; Xu, H.; Cha, J. A. K.; Wong, P. C. L.; Wen, G.; Zhang, X.; Jing, X.; Wang, F.; Tang, B. Z. *Chem. Mater.* **2000**, *12*, 2617–2624. (b) Corriu, R. J. P.; Devylder, N.; Guerin, C.; Henner, B.; Jean, A. *J. Organomet. Chem.* **1996**, *509*, 249–257. (c) Häußler, M.; Zheng, R.; Lam, J. W. Y.; Tong, H.; Dong, H.; Tang, B. Z. *J. Phys. Chem. B* **2004**, *108*, 10645–10650. (d) Miinea, L. A.; Sessions, L. B.; Ericson, K. D.; Glueck, D. S.; Grubbs, R. B. *Macromolecules* **2004**, *37*, 8967–8972. (e) Grubbs, R. B. *J. Polym. Sci., Part A: Polym. Chem.* **2005**, *43*, 4323–4336. (f) Scholz, S.; Leech, P. J.; Englert, B. C.; Sommer, W.; Weck, M.; Bunz, U. H. F. *Adv. Mater.* **2005**, *17*, 1052–1055. (g) Corbierre, M. K.; Beerens, J.; Lennox, R. B. *Chem. Mater.* **2005**, *17*, 5774–5779. (h) Johnson, B. F. G.; Sanderson, K. M.; Shephard, D. S.; Ozkaya, D.; Zhou, W. Z.; Ahmed, H.; Thomas, M. D. R.; Gladden, L.; Mantle, M. *Chem. Commun.* **2000**, 1317–1318. (i) Zhang, T.; Drouin, M.; Harvey, P. D. *Inorg. Chem.* **1999**, *38*, 957–963. (j) Keller, T. M.; Qadri, S. B. *Chem. Mater.* **2004**, *16*, 1091–1097.
- (17) Berenbaum, A.; Lough, A. J.; Manners, I. *Organometallics* **2002**, *21*, 4415–4424.
- (18) The ceramic yields of PFS **1**, **2**, and **3** at 700 °C are 37, 27, and 85%, respectively.

**Scheme 2. Generation of Ordered Arrays of PFS NRs and Subsequent Pyrolysis to Give Magnetic Ceramic NRs**

nanorods (NRs) with precisely controllable dimensions and aspect ratios by nanoimprinting a high molecular weight metallopolymer (**3** in Scheme 1) using AAO templates (Scheme 2).<sup>19,20</sup> The keys to the method we describe are that full infiltration of the precursor in the nanochannels is possible using our solventless procedure and that upon pyrolysis, the resulting ceramic NRs can precisely replicate the size and shape of their PFS precursor NRs in the template. This method also takes advantage of the unique ability to tailor the dimensions of AAO templates simply by tuning the electrochemical parameters, which is not accessible using conventional lithographic techniques.

Ordered arrays of PFS **3** NRs (Figure 1a) were achieved by capillarity-driven infiltration of PFS **3** melt into the nanoporous AAO template (Scheme 2).<sup>13</sup> In practice, an AAO template was directly pressed on the top of the polymer film (ca. 20  $\mu\text{m}$  in thickness) on a Si substrate with a known weight in air. In an oven under air, the assembly was heated to a temperature (ca. 150  $^{\circ}\text{C}$ ) above the glass transition temperature of PFS **3** ( $T_g = 89\text{ }^{\circ}\text{C}$ ) to make the polymer chains sufficiently mobile, and was then maintained for various lengths of time in air at ambient temperature. The polymer melt entered the pores of the template mainly via capillary action.<sup>21</sup> After being cooled to room temperature, the AAO template was completely removed by NaOH aqueous solution (1 M). Highly ordered arrays of polymer NRs with uniform diameter and length over large areas on a residual PFS film were obtained (see Figure S1 in the Supporting Information).

**Figure 1.** Large area highly ordered arrays of PFS NRs and their consequent ceramic NRs prepared by pyrolysis at 700  $^{\circ}\text{C}$  for 5 h: (a, b) SEM top-view images, and (c, d) angle view images.**Table 1.** Average Diameters ( $D$ ) and Lengths ( $L$ ) of PFS NRs and Ceramic NRs Prepared with an AAO Template

	AAO template	PFS NRs	ceramic NRs	
			fast ramp <sup>a</sup>	slow ramp <sup>b</sup>
$D$ (nm)	55	55	52	54
$L$ (nm)	150	85	79	150

<sup>a</sup> fast ramp = 15  $^{\circ}\text{C}/\text{min}$ . <sup>b</sup> slow ramp = 2  $^{\circ}\text{C}/\text{min}$ .

The diameter ( $D$ ) and length ( $L$ ) of the PFS NRs could be controlled by using AAO templates with different pore diameters and lengths, which were adjusted to the desired dimension by wet-chemical etching and anodization time, respectively. For example, as shown in SEM images a and c in Figure 1 and in Figures S1a of the Supporting Information, large area ordered arrays of PFS **3** NRs with an aspect ratio of ca. 1.5 ( $D = 55$  nm,  $L = 85$  nm, determined by SEM and AFM cross-sectional analysis, respectively) were achieved by nanoimprinting PFS **3** at 150  $^{\circ}\text{C}$  for 30 min using a template ( $D = 55$  nm,  $L = 150$  nm) (Table 1). NRs with the same diameter and higher aspect ratio were obtained by simply using templates with longer channels, as shown in Figure S2 of the Supporting Information, or by adjusting the heating time or temperature to partially infiltrate PFS **3** into one template, as shown in Figure S3 of the Supporting Information.

It should be noted that below 150  $^{\circ}\text{C}$ , the longest observed NRs were about one-third shorter than the pore length of the templates. This result indicates that the polymer melt does not completely fill the entire volume, presumably due to the compressed air trapped in the nanochannels.<sup>13b</sup> As discussed below, we also found that the templates can be almost completely filled.

To prepare ceramic NRs, the Al layer of AAO template was first completely removed with saturated  $\text{HgCl}_2$  aqueous solution (Scheme 2), due to the low melting point of Al (660  $^{\circ}\text{C}$ ). PFS **3** precursor NRs on the residual polymer film with the remaining  $\text{Al}_2\text{O}_3$  template were pyrolyzed at different temperatures from 500 to 800  $^{\circ}\text{C}$  in a tube furnace. A  $\text{N}_2/\text{H}_2$  (95%/5%) reductive atmosphere was used for pyrolysis to minimize the oxidation of resulting ceramics and Fe NPs by the trapped air in the nanochannels and oxygen released from AAO templates during pyrolysis. After the samples cooled to room temperature slowly,

(19) We have previously reported the generation of pillared arrays of magnetic wires using AAO templates via the incorporation of a network-forming monomer followed by ROP and pyrolysis. The procedure is much less simple than that reported here, which uses a thermoplastic linear PFS. See: Ginzburg, M.; Fournier, S.; Coombs, N.; Ozin, G. A.; Manners, I. *Chem. Commun.* **2002**, 3022–3023.

(20) Ceramic SiC-based nanomaterials such as nanotubes and bamboo-type structures have been prepared by using AAO templates and various infiltration techniques. See: (a) Wang, H.; Li, X.-D.; Kim, T.-S.; Kim, D.-P. *Appl. Phys. Lett.* **2005**, *86*, 173104. (b) Cheng, Q.-M.; Interrante, L. V.; Lienhard, M.; Shen, Q.; Wu, Z. *J. Eur. Ceram. Soc.* **2005**, *25*, 233–241. (c) Yen, H.-M.; Jou, S.; Chu, C.-J. *Mater. Sci. Eng., B* **2005**, *122*, 240–245.

(21) Zhang, M.; Dobriyal, P.; Chen, J.-T.; Russell, T. P. *Nano Lett.* **2006**, *6*, 1075–1079.



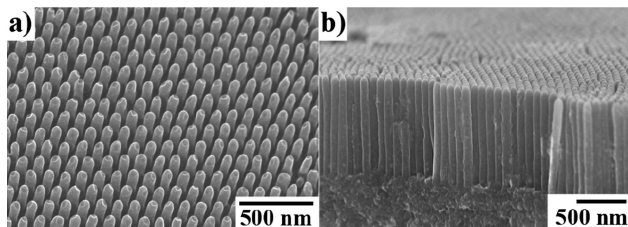


**Figure 2.** SEM image of ceramic NRs prepared at 700 °C for 5 h with temperature ramp of 2 °C/min: (a)  $D = 55$  nm,  $L = 150$  nm angle view, using a template with  $D = 55$  nm,  $L = 150$  nm; (b)  $D = 95$  nm,  $L = 1$   $\mu$ m cross-sectional view, using a template with  $D = 95$  nm,  $L = 1$   $\mu$ m.

black ceramic thin films were obtained. The  $\text{Al}_2\text{O}_3$  template was then removed by saturated NaOH solution. For pyrolyses above 700 °C, the AAO template crystallized to  $\theta$ - $\text{Al}_2\text{O}_3$  and became rather insoluble.

Images b and d in Figure 1 and Figure S1b in the Supporting Information show the representative SEM images of highly ordered arrays of ceramic NRs on the top of residual ceramic films prepared from their precursor NRs with aspect ratio of 1.5 (images a and c in Figure 1 and Figure S1a in the Supporting Information) after pyrolysis at 700 °C for 5 h with a rapid temperature ramp of 15 °C/min. Comparison of the SEM images (Figure 1) and AFM cross-section analysis results before and after pyrolysis revealed excellent shape retention of the ceramic NRs with a small contraction of the average  $L$  and  $D$  values (Table 1). As mentioned above, when prepared at 150 °C, the polymer NRs only partially filled the nanochannels. We found under the same pyrolysis conditions, but with a slower temperature ramp (2 °C/min), the  $D$  and  $L$  value of resulting ceramic NRs were consistent with those of the template, indicating complete filling of the nanochannels (Table 1 and Figure 2a). Presumably, the slow ramp allows for further infiltration before the polymer melt is ceramized and also for trapped air to be released. With a slower ramp, ceramic NRs with uniform  $L$  up to 1  $\mu$ m can be achieved (Figure 2b).

The high fidelity of this template replication method is mainly due to the remarkably high ceramic yield of PFS **3**.<sup>18</sup> For comparison, low ceramic yield PFSs **1** and **2** under the same conditions gave magnetic ceramics without any shape retention.<sup>18</sup> AAO templates also play an essential role for good shape retention by preventing the escape of volatile fragments and thereby increasing ceramic yields.

Previous studies showed that pyrolysis of PFSs either in bulk or confined to the channels of mesoporous silica yields ceramic materials containing magnetic  $\alpha$ -Fe NPs embedded in a  $\text{C}/\text{SiC}/\text{Si}_3\text{N}_4$  matrix.<sup>15</sup> The size of the Fe NPs increased with pyrolysis temperature, and their magnetic properties were thereby altered from superparamagnetic to ferromagnetic. A similar composition for the NRs formed by the AAO template method was confirmed by energy-dispersive X-ray (EDX) line scan elemental mapping. The NRs prepared at 600 °C over 5 h contained both Fe and Si (ratio ca. 1: 1, consistent with the ratio in the PFS precursor) but no O, which indicated that Fe rather than  $\text{Fe}_x\text{O}_y$  NPs are formed (see Figure S5 in the Supporting Information). A similar ability to alter magnetic properties was also noted for the AAO method. Thus, small NPs of size <5 nm in the ceramic NRs began to form at 600 °C. Pyrolysis of bulk PFS **3** under the same conditions gave small Fe NPs of

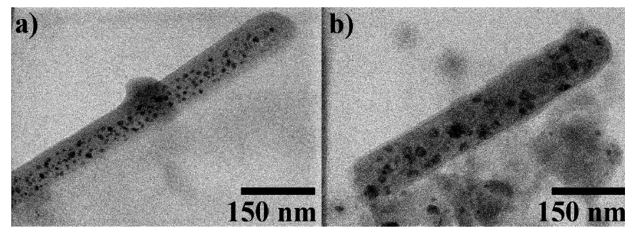


**Figure 3.** TEM images of ceramic NRs prepared at 700 °C with widths of (a) 55 and (b) 95 nm.

similar size (see Figure S6a in the Supporting Information). As the temperature was further increased to 700 °C, pyrolysis of bulk PFS **3** yielded large, irregularly shaped Fe NPs with an average size of  $32.5 \pm 12.0$  nm and a broad size distribution (see Figure S6b in the Supporting Information). Interestingly, we found the Fe NPs formed in the nanochannels with  $D = 55$  nm and  $L = 1$   $\mu$ m were much smaller (average size =  $8.2 \pm 2.4$  nm) and had a narrow size distribution and a spherical shape (Figure 3a). This result suggested the growth of the NPs was confined by the diameter of nanochannels.<sup>22</sup> To examine this hypothesis, we prepared ceramic NRs (Figure 2b) under the same conditions, but in a template with wider pores ( $D = 95$  nm). As expected, TEM analysis of this sample (Figure 3b) showed the average size of Fe NPs increased to  $20.9 \pm 4.9$  nm, while still being smaller than that of bulk sample. A significant enhancement of the magnetic properties for wider ceramic NRs compared to narrow NRs was confirmed by magnetic force microscopy (see Figure S7 in the Supporting Information). This enhancement is probably caused by the fact that as the size of NPs increased with the width of NRs, the Fe NPs would be expected to change from superparamagnetic to ferromagnetic because the theoretical single-domain size for spherical  $\alpha$ -Fe NPs is ca. 14 nm.<sup>23</sup>

In summary, we have demonstrated the fabrication of large area ordered arrays of magnetic ceramic NRs with excellent shape retention by pyrolysis of a PFS precursor in AAO templates. We are currently extending this work to diblock copolymers where one block is a high-ceramic-yield inorganic polymer that generates a hard template during pyrolysis,<sup>24</sup> and the other block has a high metal content,<sup>25</sup> and acts as a precursor to hard magnetic NPs such as FePt.<sup>26</sup>

**Acknowledgment.** We thank Dr. S. Petrov and D. A. Rider for experimental assistance.

**Supporting Information Available:** Experimental section; SEM, TEM, and AFM images; EDX line scans (PDF). This material is available free of charge via the Internet at <http://pubs.acs.org>.

CM900164B

- (22) A similar result was observed for the pyrolysis of PFS in mesoporous silica, see ref 15c.
- (23) Leslie-Pelecky, D. L.; Rieke, R. D. *Chem. Mater.* **1996**, *8*, 1770–1783.
- (24) (a) Nghiem, Q. D.; Kim, D. J.; Kim, D.-P. *Adv. Mater.* **2007**, *19*, 2351–2354. (b) Malenfant, P. R. L.; Wan, J.; Taylor, S. T.; Manoharan, M. *Nat. Nanotechnol.* **2007**, *2*, 43–46.
- (25) Chan, W. Y.; Clendenning, S. B.; Berenbaum, A.; Lough, A. J.; Manners, I.; Aouba, S.; Ruda, H. E. *J. Am. Chem. Soc.* **2005**, *127*, 1765–1772.
- (26) Liu, K.; Ho, C. L.; Aouba, S.; Zhao, Y.-Q.; Lu, Z.-H.; Petrov, S.; Coombs, N.; Dube, P.; Ruda, H. E.; Wong, W.-Y.; Manners, I. *Angew Chem., Int. Ed.* **2008**, *47*, 1255–1259.